# HYBRID MODE ANALYSIS OF RF CHARACTERISTICS IN INTEGRATED OPTICAL MODULATORS ON III-V SEMICONDUCTORS

I-6

by

Ke Wu*, Cheuk-yu Edward Tong** and Ruediger Vahldieck*

*Department of Electrical and Computer Engineering
University of Victoria, P.O. Box 1700
Victoria, B.C., V8W 2Y2
Canada, Tel. (604)721-8679

**Communications Research Laboratory
2-1 Nukui-Kitamachi 4-chome
Koganei-shi, Tokyo
184 Japan

## Abstract

The method of lines has been applied to study the RF/-microwave characteristics of III-V semiconductor traveling wave electrooptic modulators. Double-rib, multilayer strip wave-guides have been investigated. It is found that Schottky barrier junction controlled structures support multi-nondispersive modes having phase velocities that closely match the optical carrier. These modes are potentially useful in ultra-fast modulators operating into the millimeter wave band.

## INTRODUCTION

High-speed integrated electro-optic modulators and switches are fundamental building blocks of wideband lightwave communication systems and future ultra-fast signal processing technology. Much work has been done to develop efficient, low-loss, broadband phase/intensity modulators in which the coherent optical carrier is modulated by an RF/microwave signal, the spectrum of which extends up to the millimeter-wave band [1].

Classical modulators were built on lithium niobate substrates [7]. However, with recent improvement in III-V epitaxial technologies, substrate qualities and superlattice techniques to pin defects, modulators based on III-V semiconductor are currently receiving more attention [9,10]. These materials, GaAs in particular, offer the obvious advantages of technological maturity and potential monolithic integration with optic and electronic devices in Optic Electronic Integrated Circuits (OEIC). Moreover, in GaAs, there is a better velocity match between the optical carrier and the microwave modulating signal [11] so that much wider bandwidth is conceivable using traveling-wave electrodes. Eventually, III-V compounds may replace $LiNbO_3$ in the realization of electrooptic modulators.

In this paper, we present a theoretical study of the microwave properties of strip wave- guide traveling-wave modulators on III-V substrates. This theoretical characterization is essential to the design of modulators, the performance of which critically depends on their geometry [12]. Special attention is given to the reduction of the difference between the optical and microwave velocities, the key to achieving ultra-wide bandwidth [11].

To minimize the difference between the effective refraction index of the guided optical mode $N_o$ (assuming single model propagation) and the effective index of the microwave modulating signal Nm, |No-Nm|, two techniques have been used [13-15]. The first technique employs periodic electrodes to slow down the modulating signal. The second introduces material of lower microwave dielectric constant near the electrodes to reduce Nm. Using a rigorous full-wave analysis based on the method of lines [16,17], our study aims primarily at the second structure but can readily be extended to include the first one. Such a rigorous approach is necessary because the simple quasi-static analysis employed by most authors is insufficient to deal with modulating signals extending up to millimeter-wave frequencies. Multilayer substrates support a dispersive hybrid-mode which can only be analyzed through a full-wave approach.

### Structures Under Investigation

A large variety of modulator structures have been explored but the Mach-Zehnders and the directional coupler type seem to be most promising [3,8,11]. Fig. 1 shows 2 configurations adapted to III-V semiconductors [19]. Both configurations are characterized by:

- use of ribs to define the optical waveguide by geometrical lateral confinement
- low optical coupling between the 2 parallel optical waveguides [20]
- presence of depletion layers associated with the biased barrier junctions, that generate the intense DC electric field needed for the electrooptic effect
- exploitation of vertical electric field ($E\perp$) to induce phase shift.



CH2848-0/90/0000-0289$01.00 © 1990 IEEE

Both structures can be described as a generalized coupled slab multilayer waveguide. Fig. 2 gives the configuration used in our analysis.

It should be noted that as a result of doping, the dielectric permittivity of each layer assumes a complex value. Furthermore, the externally applied DC bias changes the depth of the insulating layer in the p-i-n modulator and that of the depletion layer in the Schottky barrier type modulator.

## Formulation

The linearly independent TM and TE potential functions $\psi^e$ and $\psi^h$ must satisfy Sturm-Liouville and Helmholtz equations.

$$\frac{\partial^2\psi^e}{\partial y^2} + \epsilon_r(x)\frac{\partial}{\partial x}\left[\frac{1}{\epsilon_r(x)}\cdot\frac{\partial\psi^e}{\partial x}\right] + \left[\epsilon_r(x)k_0^2 - \beta^2\right]\psi^e = 0$$

$$\frac{\partial^2\psi^h}{\partial y^2} + \frac{\partial^2\psi^h}{\partial x^2} + \left[\epsilon_r(x)k_0^2 - \beta^2\right]\psi^h = 0.$$

where

$$k_0^2 = \omega_0^2\mu_0\epsilon_0.$$

Note that the permittivity $\epsilon_r(x)$ is complex. In our structure, except for the inhomogeneous layers 4 and 5 (see Fig. 2) which contain the rib structure, this function is x-independent. The unknown propagation constant $\beta$ is also complex and is equal to $\beta_m - j\alpha_m$. Note that by imposing either magnetic or electric wall symmetry, we need to consider half of the structure only. To reduce memory size and CPU time, non-equidistant discretion is used [17].

The first step in the MOL procedure is to uncouple equations (1) and (2). This has been shown for homogeneous layers [16]. For inhomogeneous layers, however, this process is more involved and has not been published before. To begin with, the second term of Sturm-Liouville equation can be expressed, in the discretized domain as:

$$\underline{\underline{r}}^{e-1}\left\{h_0^2\epsilon_r(x)\frac{\partial}{\partial x}\left(\frac{1}{\epsilon_r(x)}\cdot\frac{\partial\psi^e}{\partial x}\right)\right\} \longrightarrow -\underline{\underline{\epsilon_r^e}}\cdot\underline{\underline{D_x}}^t\cdot\underline{\underline{\epsilon_r}}^{h^{-1}}\cdot\underline{\underline{D_x}}\cdot\underline{\phi^e} \qquad (1)$$

where $\underline{\underline{\epsilon_r^e}}$ and $\underline{\underline{\epsilon_r^h}}$ are diagonal matrices, the diagonal elements of which are the complex permittivities associated with the corresponding $e-$ or $h-$ lines. In contrast to the procedure in a homogeneous layer, now a double orthogonal transform is necessary to uncouple the equations. Besides the matrices $\underline{\underline{T^e}}$ and $\underline{\underline{T^h}}$, [16] we introduce the matrices $\underline{\underline{P^e}}$ and $\underline{\underline{P^h}}$ such that

$$\begin{aligned}\underline{\phi^e} &= \underline{\underline{T^e}}.\underline{\underline{P^e}}.\underline{V^e}\\ \underline{\phi^h} &= \underline{\underline{T^h}}.\underline{\underline{P^h}}.\underline{V^h}\end{aligned} \qquad (2)$$

After some manipulations, equation (1) and (2) becomes

$$\frac{d^2\underline{V^e}}{dy^2} - \left\{\underline{\underline{P}}^{e-1}\left[\frac{\underline{\underline{\tilde{\epsilon}_r^e}}\cdot\underline{\underline{\delta}}^t\cdot\underline{\underline{\tilde{\epsilon}_r}}^{h^{-1}}\cdot\underline{\underline{\delta}}}{h_0^2} - \underline{\underline{\tilde{\epsilon}_r^e}}k_0^2\right]\underline{\underline{P^e}} + \beta^2\right\}\underline{V^e} = 0$$

$$\frac{d^2\underline{V^h}}{dy^2} - \left\{\underline{\underline{P}}^{h^{-1}}\left[\frac{\underline{\underline{\delta}}\cdot\underline{\underline{\delta}}^t}{h_0^2} - \underline{\underline{\tilde{\epsilon}_r^h}}k_0^2\right]\underline{\underline{P^h}} + \beta^2\right\}\underline{V^h} = 0, \qquad (3)$$

where

$$\begin{aligned}\underline{\underline{\tilde{\epsilon}_r^e}} &= \underline{\underline{T^{et}}}\cdot\underline{\underline{\epsilon_r^e}}\cdot\underline{\underline{T^e}}\\ \underline{\underline{\tilde{\epsilon}_r^h}} &= \underline{\underline{T^{ht}}}\cdot\underline{\underline{\epsilon_r^h}}\cdot\underline{\underline{T^h}}\end{aligned} \qquad (4)$$

More details of the individual steps will be given in the full paper. Following the MOL procedure leads finally to a field current matrix equation at the strip discontinuity in the transformed domain.

$$\begin{pmatrix}\underline{\tilde{E}_x}\\ \underline{\tilde{E}_z}\end{pmatrix} = \begin{pmatrix}\underline{\underline{\tilde{Z}_{xx}}} & \underline{\underline{\tilde{Z}_{xz}}}\\ \underline{\underline{\tilde{Z}_{zx}}} & \underline{\underline{\tilde{Z}_{zz}}}\end{pmatrix}\cdot\begin{pmatrix}\underline{\tilde{J}_x}\\ -j\underline{\tilde{J}_z}\end{pmatrix}. \qquad (5)$$

On reverting back to the original discretized domain, a non-trivial solution of $\beta$ can be obtained when we consider that the electric field components on the strip should be set to zero, i.e.

$$\mathrm{Det}\begin{pmatrix}\underline{\underline{Z_{xx}}} & \underline{\underline{Z_{xz}}}\\ \underline{\underline{Z_{zx}}} & \underline{\underline{Z_{zz}}}\end{pmatrix}_{\text{strip}} = 0. \qquad (6)$$

## Results and Discussions

The performance of the p-i-n modulator is presented in Fig. 3 and 4 in terms of the variation of RF refractive index $N_m$, propagation loss $\alpha$ (dB/mm) and PMR with respect to frequency. $N_m$ turns out to be much greater than the optical index $N_o$=3.41 (Fig. 4). This is the cause of the limit in bandwidth. It can be seen that the reverse bias slightly improves the performance, while the difference in propagation loss is negligible. From Fig. 4, we deduce that the 3 dB bandwidth of the modulator is about 7 GHz for $L$ = 1 cm. Although this structure may be refined to improve the bandwidth, the extremely high loss towards higher frequencies would

certainly prevent the modulator to be effective in the millimeter-wave band.

In contrast to the p-i-n modulators, the Schottky-barrier controlled GaAs modulators possesses a nearly non-dispersive microwave refractive index $N_m$. This is shown in Fig. 5 for the fundamental mode at zero bias voltage. The reverse bias greatly enhances this characteristic, also shown in Fig. 5 for the first four modes, and it reduces the loss. For $V_g$ = -5$V$, the loss can be kept to below 4 db/mm at $f$ = 40 GHz (refer to Fig. 6).

However, what is most interesting is that under reverse bias, a number of nondispersive modes can exist simultaneously in the GaAs modulator. Two of these modes have refractive indices $N_m$ approaching that of the bulk modulator ($N_m$ = 3.613). This phenomenon can be explained by the fact that in a multi-layer structure, each layer may have its distinct behavior. It is well known that doped semiconductor substrates support mainly slow wave modes ($N_m > 6.0$), on the other hand, a strip deposited on a depletion layer lends itself to the propagation of dielectric waves ($N_m < \sqrt{\epsilon_r}$). Clearly, the coupling between the strip and the different layers can produce intermediate modes with ($\sqrt{\epsilon_r} < N_m <$ 6.0). The fact that the modes with lower $N_m$ possess extremely low loss (< 0.2 dB/mm) up to 40 GHz supports the argument that they are predominantly strip propagation modes.

## Conclusion

The microwave characteristics of III-V semiconductor traveling wave electrooptic modulators have been studied in a rigorous manner using the method of lines.

Both p-i-n junction and Schottky- barrier junction controlled modulators have been studied using the method of lines.

In both modulators, an external DC reverse bias can significantly reduce the transmission loss. In many cases, the reverse bias can increase the modulator bandwidth via phase velocity matching. Our numerical results show that p-i-n modulators have relatively narrow bandwidth (~7 GHz) with a minimum loss of 1.3 dB/mm. As for the Schottky-barrier controlled devices, we discover that multi-nondispersive modes can propagate simultaneously. Among these modes, some modes exhibit a low microwave refractive index that matches the optical index quite well in addition to relatively low loss. This property can be exploited to produce modulators operating into the millimeter-wave band (BW ≥ 50 GHz).

## REFERENCES


[1] Koroty S.K., Eisenstein G., Tucker R.S., Veselka J.J., Raybon G., "Optical intensity modulation to 40 GHz using a waveguide electro-optic switch," *Appl. Phys. Lett.*, vol. 50(23), pp. 1631-1633, 1987.

[2] Kishino K., Aoki S., Suematsu Y., "Wavelength variation of 1.6 $\mu$m wavelength buried heterostructure GaInAsP/InP lasers due to direction modulation," *IEEE J. Quantum Electron.*, vol. QE-18(3),pp. 343-351, 1982.

[3] Gee C.M., Thurmond G.D., Yen H.W., "17-GHz bandwidth electro-optic modulator," *Appl. Phys. Lett.*, vol. 43(11), pp. 998-1000, 1983.

[4] Kubota K., Noda J., Mikami O., "Traveling wave optical modulator using a directional coupler $LiNbO_3$ Waveguide," *IEEE J. Quantum Electron* , vol. QE-16(7), pp. 754-760, 1980.

[5] Alferness R.C., Economou N.P., Buhl L.L., "Fast compact optical waveguide switch modulator," *Appl. Phys. Lett.*, vol. 38(4), pp. 214-217, 1981.

[6] Kaminow I.P., Turner E.H., "Electrooptic light modulators," *Proc. IEEE*, vol. 54(10), pp. 1374-1390, 1966.

[7] Thylén L., "Integrated optics in $LiNbO_3$: recent developments in devices for telecommunications," *J. Lightwave Technol.*, vol. LT-4(6), pp. 847-861, 1988.

[8] Thioulouse P., Carenco A., Guglielmi R., "High speed modulation of an electrooptic directional coupler," *IEEE J. Quantum Electron.*, vol. QE-17(4), pp. 535-541, 1981.

[9] Wang S.Y., Lin S.H., "High speed III-V electrooptic waveguide modulators at $\lambda$=1.3 $\mu$m," *J. Lightwave Technol.*, vol. LT-6(6), pp. 758-771, 1988.

[10] Lengyel G., "GaAlAs p-i-n junction waveguide modulator," *J. Lightwave Technol.*, vol. LT-1(1), pp. 251-255, 1983.

[11] Alferness R.C., "Waveguide electrooptic modulators," *IEEE Trans. Microwave Theory Techn.*, vol. MTT-30(8), pp. 1121-1137, 1982.

[12] Atsuki K., Yamashita E., "Transmission line aspects of the design of broad-band electrooptic traveling-wave modulators," *J. Lightwave Technol.*, vol. LT-5(3), pp. 316-319, 1987.

[13] Lee H.Y., Itoh T., "GaAs traveling-wave optical modulator using a modulated coplanar strip electrode with periodic cross-tie overlay," *Int. J. IR & MM Waves*, vol. 10, pp. 321-335, 1989.

[14] Kaminow I.P., Liu J., "Propagation characteristics of partially loaded two-conductor transmission line for broadband light modulators," *Proc. IEEE*, vol. 51, pp. 132-136, 1963.

[15] Alferness R.C., Korotky, Marcatili E.A.J., "Velocity-matching techniques for integrated optic traveling wave switch/modulators," *IEEE J. Quantum Electron.*, vol. QE-20(3), 1984.

[16] Schulz U., Pregla R., "A new technique for analysis of the dispersion characteristics of planar waveguides," *Arch. Elek. Übertragung*, vol. 34, pp. 169-173, 1980.

[17] Diestel H., Worm S.B., "Analysis of hybrid field problems by the method of lines with nonequidistant discretization," *IEEE Trans. Microwave Theory Tech.*, vol. MTT-32(6), pp. 633-638, 1984.

[18] Pregla R., Koch M., Pascher W., "Analysis of hybrid waveguide structures consisting of microstrips and dielectric waveguides," *17th European Microwave Conf. (Rome)*, pp. 927-932, 1987.

[19] Wang S.Y., Lin S.H., Houng Y.M., "GaAs traveling-wave polarization electro-optic waveguide modulator with bandwidth in excess of 20 GHz at 1.3$\mu$m," *Appl. Phys. Lett.*, vol. 51(2), pp. 83-85, 1987.

[20] Haga H., Izutsu M., Sueta T., "$LiNBO_3$ traveling-wave light modulator/switch with an etched groove," *IEEE J. Quantum Electron.*, vol. QE-22(6), pp. 902-906.

[21] Sze S.M., *Physics of semiconductor devices*, John Wiley & Sons, 1981.

[22] Young B., Itoh T., "Effects of insulating dielectric layers in millimeter-wave planar transmission lines," *17th European Microwave Conf. (Rome)*, pp. 687-692, 1987.

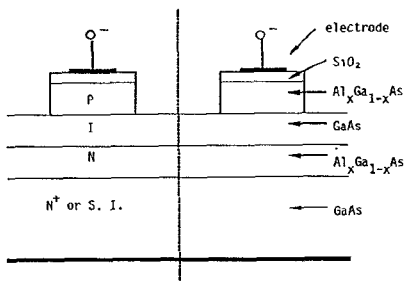


*p-i-n* type modulator

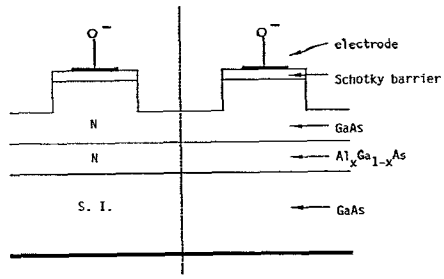


Schottky barrier type modulator.

Fig. 1 Double-hib barrier junction type GaAs electrooptic modulators

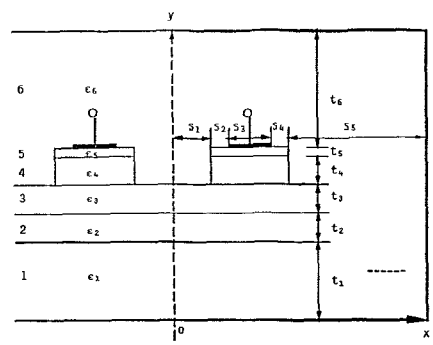


Fig. 2 General configuration of coupled slab multilayer waveguide as used in our calculations.

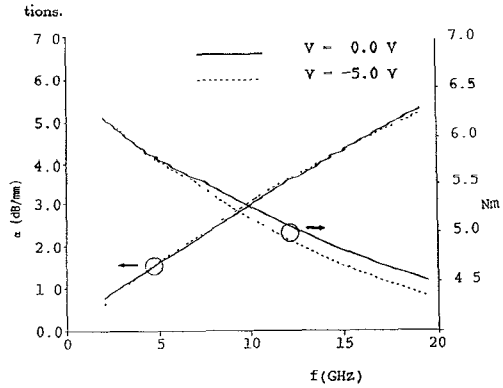


Fig. 3 Variation of the microwave refractive index $N_m$ and attenuation of modulating signal versus frequency in the p-i-n type modulator.

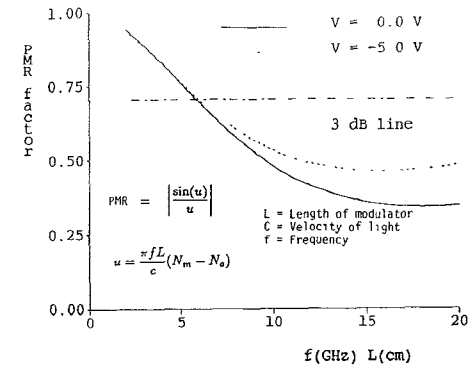


Fig. 4 Phase-modulation reduction (PMR) factor of the *p-i-n* type modulator

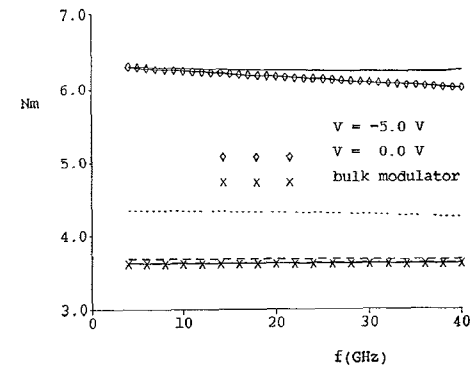


Fig. 5 Dispersion characteristics of the Schottky barrier type modulator

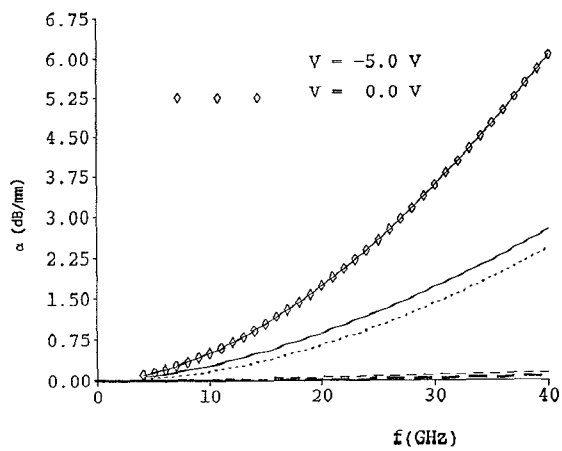


Fig. 6 Propagation loss in the Schottky barrier type modulator